

Published in final edited form as:

*Anal Chem.* 2005 February 1; 77(3): 797–805.

## Single-Chain Fragment Variable Antibody Piezoimmunosensors

Zhihong Shen<sup>†</sup>, Gabrielle A. Stryker<sup>‡</sup>, Ray L. Mernaugh<sup>§</sup>, Lei Yu<sup>†</sup>, Heping Yan<sup>§</sup>, and Xiangqun Zeng<sup>†\*</sup>

<sup>†</sup>*Department of Chemistry, Oakland University, Rochester, Michigan 48309*

<sup>‡</sup>*Department of Biological Sciences, Oakland University, Rochester, Michigan 48309*

<sup>§</sup>*Department of Biochemistry, School of Medicine, Vanderbilt University, Nashville, Tennessee 37232*

### Abstract

In this paper, we describe a novel nonlabeled biosensor with high diagnostic potential for rapid and sensitive detection of antigens in complex biological samples. The biosensor comprises a piezoimmunosensor (PZ) displaying a specially constructed recombinant antibody on its surface. The recombinant single-chain fragment variable (scFv) antibody contained a cysteine within the linker amino acid sequence used to join the scFv variable heavy and light chains. The presence of cysteine induced the scFv construct to self-assemble as a densely packed rigid monolayer on the gold surface of a quartz crystal microbalance. scFv molecules in this self-assembled mono-layer (SAM) exhibited a defined orientation and high areal densities, with scFv-modified microbalance surfaces displaying 35 times as many variable antigen-binding sites per square centimeter as surfaces modified with whole antibody. Experimental data show that the scFv SAM PZ is superior to Fab fragment, Fab fragment containing a free sulfhydryl group (i.e., Fab-SH), and whole antibody PZs regarding sensitivity and specificity. Because of their small uniform size (MW  $\approx$  27000) and the ease with which they can be modified using genetic engineering, scFv's have significant advantages over whole antibodies in microbalance biosensor systems. We demonstrate here that the use of scFv containing a cysteine within the scFv linker sequence (i.e., scFv-cys) for preparation of biosensor surfaces markedly increases the density of available antigen-binding sites, yielding a system that is highly selective, rapid, and capable of detecting low concentrations of antigens in complex samples.

Biosensor systems that detect biological and chemical agents have important medical, environmental, public safety, and defense applications. An ideal biosensor would be sensitive, rapid, reliable, robust, and inexpensive. Piezoimmunosensors (PZs) are a type of biosensor utilizing antibodies and a quartz crystal microbalance (QCM) to detect minute changes in mass as antigens bind to the antibodies on the QCM surface.<sup>1,2</sup> Although their diagnostic potential is theoretically quite high, in practice, the usefulness of PZs has been limited by the fact that typical IgG antibodies can trap or nonspecifically bind irrelevant molecules, thus yielding false positive signals in assays. Additionally, there remains some skepticism concerning their applicability as biosensors due to the complexity of the physical properties of biofilms in a liquid that make it difficult to establish an explicit relationship between the added mass and a change in the resonant frequency. The QCM gives a direct response signal that characterizes a binding event between an antibody layer, immobilized on the surface of the QCM or other transducers, and the antigen to be detected. The mass change on the QCM surface is estimated using the Sauerbrey equation,<sup>3</sup>  $\Delta f = -2\Delta m n f_0^2 / [A(\mu_q \rho_q)^{1/2}]$ , where  $n$  is the overtone number,  $\mu_q$  is the shear modulus of the quartz [ $2.947 \times 10^{11}$  g/(cm·s<sup>2</sup>)],  $\rho_q$  is the density of the quartz (2.648 g/cm<sup>3</sup>), and  $\Delta m/A$  is the areal density and assumes that the foreign mass is strongly

\*To whom correspondence should be addressed. Phone: (248) 370-2881. Fax: (248) 370-2321. E-mail: zeng@oakland.edu.

coupled to the resonator. However, this may not be the case, as several studies have demonstrated that the deposited mass is generally overestimated.<sup>4</sup> Furthermore, significant levels of nonspecific adsorption are common with QCM-based PZs since large immunoglobulin molecules immobilize onto the gold surface with low densities and random orientations. The quartz crystal microbalance is a mass sensor, so any molecule able to adsorb to the surface is a potential interfering agent. To minimize nonspecific adsorption, surfaces containing end-attached oligo(ethylene oxide) that have smaller nonspecific protein and cell adsorption were reported.<sup>5</sup> Unoccupied active surface areas were successfully blocked by some nonactive proteins (bovine serum albumin (BSA), gelatin, or casein) before binding of analyte or reduced by the addition of detergents.<sup>6,7</sup> Methods have also been described for improving the orientation of proteins on gold surfaces<sup>8,9</sup> using biotin–streptavidin binding or sandwich layers; however, problems associated with low surface protein densities and nonspecific adsorption or trapping remain.

Recombinant single-chain fragment variable (scFv) fragments are small heterodimers comprising the antibody heavy-chain ( $V_H$ ) and light-chain ( $V_L$ ) variable domains that are connected by a peptide linker to stabilize the molecule.<sup>10,11</sup> They represent the smallest functional  $V_H$ – $V_L$  domains of an antibody necessary for high-affinity binding of antigen.<sup>12</sup> Because of their small size and homogeneity, scFv's offer significant advantages over polyclonal and monoclonal antibodies for PZ immunochemical detection of antigens. For example, polyclonal antibodies are quite heterogeneous populations, with significant differences in their binding characteristics. While monoclonal antibodies afford homogeneous binding characteristics, but are quite large, nonspecific binding and contaminant trapping are more likely to occur. In contrast, scFv's (MW  $\approx$  27000)<sup>13</sup> are very small and can be coupled at high density onto a surface to reduce nonspecific contaminant trapping.

In this paper, we describe the production and use of a novel piezoimmunosensor that is self-contained and inexpensive and uses the selective recognition capacity of scFv immobilized onto its surface to rapidly detect and identify antigens in a complex sample. By taking advantage of current developments in genetic engineering (i.e., introduction of unique attachment sites on protein surfaces that orient the macromolecule in a self-assembled film<sup>14</sup>), we specially engineered the scFv (Figure 1a and Figure 2) to contain a cysteine within the scFv linker sequence so that a covalent linkage could be affected between the sulfur atom of the scFv cysteine moiety and the gold surface of the QCM, thereby generating self-assembled monolayers (SAMs).<sup>15</sup> The system we use to illustrate this concept is A10B scFv. It is typically used to develop all new methodologies simply because the expression level of genetically modified A10B scFv is quite adequate and the antigens (rabbit IgG and rabbit IgG Fab) are inexpensive, without biohazard, and can be commercially obtained and labeled with a variety of different reporter molecules (e.g., biotin, dyes, enzymes, etc.). Furthermore, the A10B scFv we used is very stable and is routinely stored frozen or unfrozen for extended periods of time with little or no loss of activity.

The A10B hybridoma cell line was used as the source of genetic information for production of scFv. This cell line produces a monoclonal IgG1 antibody that binds specifically to the constant region ( $C_H1$ ) of rabbit IgG (Figure 1b,c). To obtain the A10B scFv, synthetic oligonucleotides encoding for the GGGGSGGGGSGGGGS amino acid linker sequence were used to join the A10B  $V_H$  and  $V_L$  DNA sequences to produce the scFv construct. An *Escherichia coli* bacterial colony (designated A10B 210E) was initially picked when the A10B hybridoma monoclonal antibody was first cloned as an scFv recombinant antibody. The A10B 210E scFv expressed well and was stable upon storage. Like the parent A10B monoclonal antibody, A10B 210E scFv bound to and specifically interacted with the positive control antigen (rabbit IgG) and not with negative control antigens. DNA sequencing of the scFv confirmed the replacement of the first glycine amino acid by a cysteine (C) group (Figure 2).

The A10B 210E scFv linker sequence was CGGGSGGGGSGGGGS instead of GGGGSGGGGSGGGGS. The A10B hybridoma monoclonal antibody was cloned again as an scFv. The resulting A10B scFv contained a GGGGSGGGGSGGGGS linker.

The –SH group present on cysteine within biomolecules can be used to covalently attach biomolecules to metal (e.g., Au) surfaces. In the following study, the A10B 210E (i.e., A10B scFv-cys) was immobilized on a gold QCM to develop a piezoimmunosensor that could be used to specifically detect an antigen in a crude biological sample. The A10B scFv-cys was used to demonstrate that the scFv orientation on the sensor surface could be controlled and that nonspecific binding and contaminant trapping were significantly reduced when compared to those of surfaces immobilized with the A10B IgG monoclonal antibody, Fab fragment, or scFv without a cysteine in the linker sequence.

## MATERIALS AND METHODS

### Reagents

BSA fraction V (Catalog no. A-9418), BSA (Catalog no. A-4503), rabbit IgG (Catalog no. I-5006), goat anti-rabbit IgG (Catalog no. R-2004), carbonic anhydrase (Catalog no. C-4831), human serum albumin (HSA; Catalog no. A-1653), horseradish peroxidase (HRP; Catalog no. P-6782), and streptavidin (Catalog no. S-4762) were purchased from Sigma, Inc. Donkey anti-rabbit IgG (donkey IgG; Catalog no. 711-005-152), goat anti-human IgG (goat IgG; Catalog no. 109-005-003), and HRP-conjugated goat anti-mouse Fc  $\gamma$  (Catalog no. 115-036-071) and rabbit anti-mouse IgG Fab (Catalog no. 315-007-003) were purchased from Jackson Immunolabs. The anti-E-tag monoclonal antibody (Catalog no. 27-9412-01), HRP/anti-E-tag monoclonal antibody conjugate (Catalog no. 27-9413-01), and HRP/anti-M13 monoclonal antibody conjugate (Catalog no. 27-942-01) were purchased from Amersham. A human anti-HIV monoclonal antibody designated 17b21 (human IgG) was protein-A/G purified from a 17b21 hybridoma serum-free tissue culture supernatant. 2-Mercaptoethanolamine-HCl (Catalog no. 20408) was obtained from Pierce. Phosphate-buffered saline (PBS), pH 7.2 (Gibco BRL no. 20012-027), fetal bovine serum (Gibco BRL no. 16000-044), and all other chemicals (Aldrich) were used as received. The A10B monoclonal antibody was purified either from A10B mouse ascites fluid using caprylic acid and ammonium sulfate precipitation<sup>16</sup> or from A10B hybridoma serum-free tissue culture medium using ammonium sulfate precipitation. Purified CYP1B1 P450 was provided by Dr. Fritz Parl from Vanderbilt University. The I20 scFv specific for CYP1B1 was used as a negative control for ELISA. Fresh rabbit serum was provided by Shravan Chintala, Ph.D. (Eye Research Institute, Oakland University) and Michael Hartzler, Ph.D. (Beaumont Hospital, Royal Oak, MI). Serum samples were collected by venipuncture in the presence of heparin, centrifuged at 3000g for 10 min to pellet red blood cells, and frozen at –80 °C (The Institutional and Animal Care Use Protocols (IACUC) number was AL-03-03 with an approval date of June 30, 2003).

### HRP/A10B Monoclonal Conjugation

Purified A10B monoclonal antibody was conjugated to HRP using a modification of a previously published protocol.<sup>16</sup> Briefly, HRP was incubated with 0.1 M sodium metaperiodate and then dialyzed extensively against 1 mM sodium acetate, pH 4.4. Periodate-activated HRP was mixed with purified A10B monoclonal antibody at a ratio of 0.8 mg of HRP to 1 mg of A10B monoclonal antibody in 50 mM carbonate buffer, pH 9–9.5, for 2 h at room temperature. The A10B/HRP conjugation reaction was terminated with sodium borohydride and dialyzed against PBS.

### A10B scFv Preparation

Spleen B cells from female Balb/c mice, immunized with purified rabbit IgG, were fused to SP2/0 myeloma cells to produce the A10B hybridoma cell line. This hybridoma produces an IgG1 monoclonal antibody that specifically interacts with the C<sub>H</sub>1 domain of rabbit IgG. A10B cells were used as the source of genetic information for scFv production. mRNA was purified from approximately  $5 \times 10^6$  hybridoma cells (Amersham QuickPrep mRNA purification kit), and scFv were generated using Amersham's recombinant phage antibody system (RPAS) according to the manufacturer's instructions. The RPAS synthetic oligonucleotides encoding for the (GGGS)<sub>3</sub> linker peptide sequence were used as is without modification. All scFv's expressed using the RPAS kit are encoded within the Amersham pCANTAB5E phagemid vector, which contains an ampicillin-resistance gene to select for bacterial clones that contain the scFv-encoding phagemid. All scFv's are expressed as an epitope-E-tagged scFv. The E-tag is recognized by an anti-E-tag monoclonal antibody or HRP/anti-E-tag monoclonal antibody conjugate (Amersham Biosciences), which can be used in immunoassays (e.g., ELISAs and Western blots) to detect scFv bound to antigens. All scFv's were obtained from *E. coli* bacterial periplasmic extracts according to a previously published protocol<sup>17</sup> and affinity purified on an anti-E-tag monoclonal antibody column using the Amersham RPAS purification kit according to the manufacturer's instructions. A10B scFv purity was assessed by SDS PAGE and Western blot analysis. Western blots were probed with the HRP/anti-E-tag monoclonal antibody conjugate, according to the manufacturer's instructions, to detect E-tagged scFv's. scFv's bearing a free cysteine – SH can form disulfide bonds with a free – SH on other scFv's to form scFv dimers. However, the dimerization does not cause a problem in scFv sensor applications. The scFv disulfide adsorbs on the gold surface with cleavage of its sulfur–sulfur bond and forms a new species (a gold thiolate).<sup>18</sup>

### A10B Fab Production and Mercaptoethanolamine Reduction

Purified A10B monoclonal antibody was digested with papain<sup>19</sup> to obtain A10B Fab and Fc fragments. Digests were dialyzed against PBS. Undigested A10B monoclonal antibody and A10B Fc fragments were then removed from A10B Fab fragments using goat anti-mouse IgG Fc antibody coupled to Sepharose beads. A10B Fab fragments were subsequently reduced with 2-mercaptoethanolamine (MEA) according to the Pierce instruction manual to produce A10B Fab fragments that contain a free sulfhydryl group (i.e., Fab-SH) that could form a thiolated bond with a gold substrate.

### HRP/A10B Monoclonal Antibody and A10B scFv and scFv-cys ELISA

Individual wells of a 384-well microtiter plate were coated for 90 min at room temperature with either 50 ng of purified CYP1B1 or 500 ng of streptavidin, rabbit IgG, human IgG (17b21 human monoclonal antibody), carbonic anhydrase, human serum albumin, bovine serum albumin, or donkey antibody diluted in PBS. The wells were emptied, then filled with PBS containing 0.1% Tween 20 (PBS-T), and incubated for 15–30 min at room temperature to prevent proteins from binding nonspecifically to the microtiter wells. The wells were emptied, and HRP/A10B, HRP/anti-M13, and HRP/anti-E-tag monoclonal antibodies diluted in PBS-T were added to the antigen-coated wells. The ICELISA protocol accompanying the Amersham HRP/anti-E-tag monoclonal antibody was used to determine scFv specificity. A 25- $\mu$ L sample of anti-E-tag/HRP diluted 1:4000 in PBS-T was added to each well. A 25- $\mu$ L sample of purified scFv diluted to 0.4  $\mu$ g/mL in PBS was added to the antigen-coated wells. The microtiter plates were incubated for 1 h at room temperature and washed six times with PBS-T, and then 50  $\mu$ L of ABTS (2,2'-azinobis(3-ethylbenzthiazoline-6-sulfonic acid)) containing hydrogen peroxide was added to each well for color development. The plates were incubated at room temperature for 10–30 min. The BioTek Elx800nb plate reader operating at 405 nm was then used to determine the absorbance readings for each well.

## A10B Fab Fragment ELISA

Wells of a 384-well microtiter plate were coated with ~ 150 ng of either rabbit IgG or BSA diluted in PBS. The wells were blocked with PBS-T. Purified A10B Fab fragments either modified with MEA or unmodified were diluted (from 4 to 0.25  $\mu\text{g/mL}$ , 30  $\mu\text{L/well}$ ) in PBS-T and added to the wells. The microtiter plate was incubated for 1 h at room temperature and then washed three times with PBS-T. A 30- $\mu\text{L}$  sample of HRP-conjugated goat anti-mouse IgG  $\kappa$  light chain antibody (Southern Biotechnology Associates, Catalog no. 1050-05) diluted 1:2000 in PBS-T was added to all wells to detect A10B Fab fragments bound to rabbit IgG or BSA. After 1 h of incubation at room temperature, the wells were washed three times with PBS-T, substrate was added, and absorbance readings were determined as described previously.

## Immobilization

The nonpolished gold quartz crystal electrode (International Crystal Manufacturing Co. Inc., Oklahoma) was mounted in a custom-made Kel-F cell. It was cleaned three times using concentrated nitric and sulfuric acid (1:1 v/v), biograde water (i.e., resistance greater than 18 M $\Omega$ , and further radiated by UV light and filtered with a 0.2- $\mu\text{m}$  filter), and ethanol in series, and then the cell was dried using nitrogen. The frequency of the electrode was measured both dry and in PBS, pH 7.2. One side of the gold quartz crystal was incubated in a solution of A10B scFv-cys (0.4 mg/mL) in PBS at 4  $^{\circ}\text{C}$  for 20 h. After incubation, the electrode surface was washed with PBS and biograde water and dried under nitrogen. Any remaining sites on the scFv-cys-modified electrode were then blocked for 30 min with 0.1% BSA in PBS, after which the electrode was again washed with PBS and biograde water. Note 0.1% BSA was used as the blocking reagent since it showed better performance than methoxypoly(ethylene glycol) thiol (PEG) (NEKTAR Transforming Therapeutics, Catalog no. 2M4D0H11) and chick egg albumin (Sigma, Catalog no. A5503-1G) tested in our sensor as it is often used in traditional immunoassays.<sup>20</sup> Electrodes with immobilized A10B monoclonal antibody, A10B scFv without cysteine, A10B Fab, and A10B Fab-SH were prepared similarly.

## QCM Measurement

AT-cut 10-MHz quartz crystals (non-polished with ~1000  $\text{\AA}$  of gold, geometric area 0.23  $\text{cm}^2$ , International Crystal Co., Oklahoma) were used throughout the study. One side of the gold electrode was oriented toward air, while the A10B scFv-cys-modified side was mounted in the Kel-F cell and immersed in 1 mL of PBS. The cell was placed in a Faraday cage, and various concentrations of rabbit IgG were added in 20- $\mu\text{L}$  aliquots with stirring. The change in frequency and series damping resistance of the QCM were monitored simultaneously using a network/spectrum/impedance analyzer (Agilent 4395A) controlled by a PC via an Intel card.

## Electrochemical Characterization

The gold electrode of the QCM with immobilized scFv was used as a working electrode. Platinum wire and a saturated calomel electrode (SCE) were used as counter and reference electrodes, respectively. Cyclic voltammetry and electrochemical impedance spectroscopy were carried out in a solution of 0.1 M NaClO<sub>4</sub> containing 1 mM K<sub>3</sub>Fe(CN)<sub>6</sub>/K<sub>4</sub>Fe(CN)<sub>6</sub> using a PARSTAT 2263 advanced electrochemical system (Princeton Applied Research).

## Rabbit Serum IgG Analysis

**(a) Sandwich ELISA**—Serum concentrations of rabbit IgG were quantitatively measured using an ELISA kit according to the manufacturer's protocol (Bethyl Laboratories, Inc., Catalog no. E120-111). Briefly, microtiter plates (Corning) were coated with affinity-purified goat anti-rabbit IgG (1  $\mu\text{g/mL}$ , Bethyl Laboratories, Catalog no. A120-111A) in 0.05 M carbonate/bicarbonate buffer, pH 9.6, and then blocked with 1% BSA in 50 mM Tris, 0.14 M



NaCl, pH 8.0. Serial dilutions of the standard rabbit reference serum (Bethyl Laboratories, Catalog no. RS10-107) or sample serum were then applied to the wells in triplicate and incubated for 60 min. HRP-conjugated goat anti-rabbit (Bethyl Laboratories, Catalog no. A120-111P) diluted 1:75 000 in 50 mM Tris, 0.14 M NaCl, 1% BSA, 0.05% Tween 20, pH 8.0, was added to the wells. The reaction was detected with 3,3',5,5'-tetramethylbenzidine and stopped at 30 min with 2 M H<sub>2</sub>SO<sub>4</sub>.

**(b) QCM Analysis**—Rabbit serum was diluted 1:100 with PBS containing 0.1% Tween-20, spiked with varying concentrations of the rabbit IgG standard, and analyzed using the A10B scFv-cys PZs. Final rabbit IgG concentrations in serum were obtained from the calibration curve in Figure 6b.

## RESULTS AND DISCUSSION

### SDS-PAGE and Western Blot Analysis of A10B scFv

E-tagged A10B scFv and scFv-cys were affinity purified by affinity chromatography using an anti-E-tag monoclonal antibody column. Affinity-purified scFv antibodies were analyzed by SDS-PAGE and Western blot analysis to determine scFv purity and integrity. Typically, the molecular weights of scFv antibodies, as ascertained by SDS-PAGE, range from 29 000 to 36 000. Under reducing conditions, purified A10B scFv and scFv-cys migrated as single bands at MW  $\approx$  33000 on SDS-PAGE (Figure 3a) and were stained with the HRP/anti-E-tag monoclonal antibody on Western blot analysis (Figure 3b). As evidenced by Western blot analysis, purified A10B scFv migrated as a single band at a MW of  $\sim$ 32 000 and did not appear to be degraded.

### Characterization of A10B Monoclonal, Fab Fragment, and scFv Antibodies by ELISA

The specificity of A10B monoclonal, Fab fragment, and scFv antibodies was determined by ELISA (Figure 4a). HRP/A10B monoclonal antibody conjugate, scFv, and scFv-cys specifically interacted with the A10B antigen (rabbit IgG) but not with negative control antigens (CYP1B1, streptavidin, human IgG, carbonic anhydrase, human serum albumin, bovine serum albumin, and donkey antibody). Negative control HRP/anti-E and HRP/anti-M13 monoclonal antibodies did not interact with positive or negative control antigens. The anti-CYP1B1 scFv (designated I20) interacted with CYP1B1 but not with rabbit IgG or other antigens assayed by ELISA. The specificity of A10B Fab fragments reduced with MEA or nonreduced was assayed by ELISA. Reduced or nonreduced A10B Fab fragments specifically interacted with A10B antigen (rabbit IgG) but not with a negative control antigen (BSA) (Figure 4b).

### Characterization of the scFv SAM Layers

The A10B scFv-cys has an E-tag incorporated into the amino terminus of the protein (E-tag: GAPVPYDPLEPR). An E-tag is a specific linear epitope recognized by commercially available HRP-conjugated anti-E-tag antibody, thus providing a means for a colorimetric assay to verify the immobilization of A10B scFv-cys on the gold surface of the sensor. If A10B scFv-cys is bound to the gold surface, the HRP label on the anti-E-tag antibody will bind and the surface will turn green when a solution of ABTS and hydrogen peroxide is added. We observed the above colorimetric change (data not shown here but in the Supporting Information file). The presence of scFv-cys on the QCM sensor surface was further verified by cyclic voltammetry (CV; Figure 5a) and electrochemical impedance (Figure 5b, Nyquist plots). All

---

**SUPPORTING INFORMATION AVAILABLE** Details of HRP immunoassay. This material is available free of charge via the Internet at <http://pubs.acs.org>.

of these methods confirmed the existence of surface scFv self-assembled monolayers or the binding of surface-immobilized scFv to its corresponding antigen. A  $K_4Fe(CN)_6/K_3Fe(CN)_6$  solution was used as an electrochemical probe to test the integrity of the scFv-cys SAM on the gold surface. Electron transfer between a species [e.g.,  $K_4Fe(CN)_6/K_3Fe(CN)_6$ ] in the solution and the electrode occurs either by tunneling through the monolayer (e.g., immobilized scFv-cys) or at a defect in the monolayer. Therefore, the extent of surface passivation to electron transfer is a useful measure of defects in the monolayer. As shown in Figure 5a, CV of the bare gold surface gave ideal  $K_4Fe(CN)_6/K_3Fe(CN)_6$  reversible redox peaks. The faradic current was dramatically attenuated on the scFv-modified surface. Subsequent exposure of these scFv SAMs to 0.1% BSA blocking reagent, followed by rabbit IgG, resulted in a further increase in passivation. Stripping of the scFv-cys monolayer by reductive desorption renewed the gold surface. Figure 5b also illustrates that the electron-transfer resistance,  $R_{et}$ , of the  $Fe(CN)_6^{IV}/Fe(CN)_6^{III}$  redox couple increases upon subsequent immobilization of scFv-cys, blocking with BSA, and binding with rabbit IgG. These experiments demonstrated that a BSA-blocked SAM of scFv-cys presents an impermeable barrier to electroactive species in aqueous electrolytes and that a primary mode of electrochemical communication between the electrode and the solution electrophore occurs at defect sites rather than by conduction through the monolayer.

### Detection of the Target Antigen (i.e., Rabbit IgG and Fab)

The scFv sensor performance was evaluated using various concentrations of rabbit IgG. The A10B scFv-cys was immobilized onto several QCM gold electrodes. The frequency change was monitored over time in the presence of increasing concentrations of rabbit IgG ( $1.7 \times 10^{-9}$  to  $1.3 \times 10^{-7}$  M) in PBS (Figure 6a). From these standard calibration data, a linear range of  $1.7 \times 10^{-9}$  to  $6.6 \times 10^{-8}$  M was obtained (Figure 6b). Solutions were stirred during IgG addition and subsequent measurement to ensure that mass transfer was not a rate-limiting step. The response is, therefore, limited only by the amount of rabbit IgG available for binding rather than by the rabbit IgG–scFv binding equilibrium.<sup>21</sup> The concentration-dependent change in the resonant frequency in this system demonstrates the potential of this technique in immunochemical analysis.

Figure 6c, curve A, depicts results obtained when secondary polyclonal goat anti-rabbit IgG was added to the QCM surface utilizing the sensor surface previously used for Figure 6a, curve A. Binding of goat anti-rabbit IgG to rabbit IgG captured by immobilized A10B scFv-cys caused an additional 2-fold decrease in frequency. When scFv's are immobilized onto the sensor surface, each molecule will capture a single rabbit IgG antibody, share the antibody with a neighboring scFv (two binding sites per rabbit antibody), or sterically interfere with binding of antibody to neighboring scFv's (Figure 1c). Polyclonal goat anti-rabbit IgG consists of a heterogeneous population of antibodies specific for a number of different epitopes or antigenic sites on rabbit IgG. Therefore, antibodies comprising this population can recognize and bind to multiple sites on a rabbit IgG molecule captured by the A10B scFv-cys monolayer on the sensor surface. As a consequence, one or two anti-rabbit antibodies may bind to one rabbit IgG captured by one A10B scFv-cys on the surface. This significantly enhances the detection limit for a sandwich immunoassay. In the absence of rabbit IgG (negative control), the addition of goat anti-rabbit antibody to biosensor generated only a very small frequency decrease owing to the low level of nonspecific adsorption (Figure 6c, curve B). These data indicate that the frequency decrease observed when rabbit IgG is applied to the biosensor is due to the specific interaction between rabbit IgG and A10B scFv-cys, and not to an interaction between goat anti-rabbit IgG and the immobilized scFv-cys.

The A10B antibody binds to the  $C_{H1}$  region of rabbit IgG (Figure 1). The  $C_{H1}$  region is located at the Fab portion of the rabbit IgG. Since Fab is only one-third the molecular weight of whole rabbit IgG, using it as the analyte will not only confirm the binding region of the analyte but

also further show the sensitivity of the scFv-cys PZ. Figure 6d shows the change of frequency vs time curve that was obtained by adding successive volumes of 13  $\mu\text{M}$  rabbit IgG Fab to the 1-mL cell. scFv-cys binding sites are almost saturated upon the third addition of rabbit IgG Fab as demonstrated by the smaller frequency shift compared to those of the first and second additions of rabbit IgG Fab. This further demonstrates that the scFv's can detect small antigens.

Using a Langmuir isotherm,<sup>22</sup> the binding constants of A10B scFv-cys with rabbit IgG and rabbit IgG Fab were determined to be  $1.9 \times 10^7$  and  $3.6 \times 10^6 \text{ M}^{-1}$ , respectively.

### Comparison of PZs with A10B scFv-cys, A10B scFv, A10B Fab, A10B Fab-SH, and Whole A10B Monoclonal Antibodies Immobilized on Their Surfaces

To compare the sensitivity and selectivity for antigen recognition in complex samples, we tested the performance of PZs prepared with A10B scFv-cys, A10B scFv (no cysteine linker), A10B Fab-SH (i.e., modified with MEA), A10B Fab (i.e., unmodified), and A10B monoclonal antibodies in the presence of fetal bovine serum (FBS), a mixture with a level of complexity similar to that encountered in biological samples. Figure 7 shows the results obtained for the five types of biosensors when 20  $\mu\text{L}$  of FBS (0.36 mg/mL total protein concentration) was added on three separate occasions. The scFv-cys-modified surface shows no detectable nonspecific absorption, while Fab-SH and Fab biosensors show some nonspecific and the scFv and monoclonal antibody biosensors show many more nonspecific interactions. Furthermore, the A10B scFv-cys biosensor has significantly higher sensitivity to rabbit IgG compared to the other four biosensors. A10B Fab fragments containing a free sulfhydryl group (i.e., Fab-SH) that forms a thiolated bond with a gold substrate show less nonspecific adsorption and higher sensitivity compared with Fab. This further proves that immobilization through Au-S interactions results in a more densely bound surface film with proper orientation. The detection limit for A10B scFv-cys binding to rabbit IgG was  $(1.1 \pm 0.4) \times 10^{-9} \text{ M}$  ( $n = 6$ ), which is lower than that of A10B Fab-SH (i.e.,  $(8.5 \pm 0.4) \times 10^{-9} \text{ M}$  ( $n = 3$ )). By using an initial rate of change measurement, concentrations in the nanomolar range can be determined within a few seconds by using the A10B scFv-cys PZ.

One problem encountered with biological sensors is the biofouling that occurs as contaminants accumulate on the sensor surface over time. On the basis of our results, this does not appear to be a problem with scFv-cys PZs. With these biosensors, the monolayer of scFv molecules on the gold QCM surface is so uniform and densely packed that the potential for nonspecific interactions or trapping of irrelevant molecules is greatly reduced. Even after three rounds of exposure to FBS, there was negligible nonspecific adsorption, indicating much lower levels of contaminant accretion than with monoclonal whole antibody PZs (Figure 7). Furthermore, the A10B scFv-cys biosensor, even after repeated exposure to FBS, retained its high sensitivity for detection of antigen in a complex matrix (Figure 7). These data demonstrate that when A10B scFv-cys molecules self-assemble as a monolayer on the surface of a microbalance, they exhibit a defined orientation and high areal densities, resulting in a more rigidly bound surface scFv film. Their high areal density preserves scFv stability and specificity, enhances scFv rigidity, inhibits nonspecific adsorption, and endows the scFv's with significant advantages over the whole antibody, antibody Fab fragment, and scFv (without cysteine linker) PZs and the ability to function better in a "dirty" environment.

### Rigidity of the Monolayers

The Sauerbrey relationship was derived by assuming that the attached film is rigid and strongly coupled to the resonator. It does not apply if the deposited film is viscoelastic. Quartz crystal resonators are known for their sensitivity to viscoelastic properties,<sup>4</sup> a characteristic that limits their application for precise mass detection of biological materials in a liquid phase. We have demonstrated the applicability of scFv-cys PZs by determining the crystal impedance of the



resonator. A QCM acoustic impedance analysis was used to determine simultaneously the crystal impedance of the resonator for the binding events shown in Figure 6a,c,d and Figure 7. When this was measured in the presence or absence of attached antibodies, changes in the series resistance in the Butterworth – Van Dyke-equivalent circuit<sup>23–25</sup> were barely detectable. The change of damping resistances in all cases was  $|\Delta R_q|/R_q \leq 1\%$  (Table 1). This suggests that the biofilms-immobilized A10B scFv, scFv-cys, Fab-SH, Fab, and monoclonal antibodies-were exhibiting rigid, rather than viscoelastic, behavior in our experiments, and consequently, the Sauerbrey equation is valid.

### Reversibility of the scFv-cys PZ

The A10B scFv-cys PZ sensor surface was easily regenerated by stripping the rabbit IgG, previously captured by the immobilized A10B scFv-cys, from the surface using an acidic solution (0.5% glacial acetic acid or 10 mM HCl). While exposure to acidic conditions did not significantly affect the immobilized A10B-scFv-cys, it did reduce the ability of A10B-scFv-cys to bind rabbit IgG. Since formation of the scFv SAM is based on the chemisorption of the linker cysteine's sulfur atom onto the gold surface— $\text{scFv-SH} + \text{gold} \rightarrow \text{scFv-gold} + \text{e}^- + \text{H}^+$ —the scFv SAM can be removed from the metal surface through a reductive desorption. Figure 5, in fact, shows that the entire antigen-scFv complex could be removed by reductive desorption using an electrochemical method. The regenerated surface was relabeled using fresh A10B scFv-cys and successfully used in a subsequent assay to detect rabbit IgG. The relabeled QCM gave a similar frequency change (i.e., 120 Hz) when rabbit IgG (20  $\mu\text{L}$ , 1 mg/mL) was added to the 1-mL PBS assay solution. Although regeneration of the biosensor was easily accomplished, we recommend that the sensors used for biohazard detection be disposed of after use to minimize contamination. Because they are inexpensive to produce, single-use biosensors are quite feasible and economical.

### Surface Coverage of the scFv-cys PZ

Figure 8 shows the stripping voltammograms obtained with a bare gold electrode in the presence of 0.5 M KOH, and with gold electrodes modified with cysteine, A10B Fab, A10B Fab-SH, or A10B scFv-cys. Cathodic peaks at  $-0.8$  and  $-1.15$  V were observed on the first potential sweep for the cysteine-modified gold electrode. Those peaks decreased gradually in the following scans and vanished after 10 scans. Cyclic voltammetry of the A10B scFv-cys- and A10B Fab-SH-modified gold electrode yielded two similar peaks, with a more negative shift in peak potential ( $-0.93$  and  $-1.17$  V). This is expected as the neighboring protein changed the chemical environment of cysteine in the A10B scFv linker or the SH in Fab fragments, resulting in a shift of reduction potentials. No peak was observed at  $-0.93$  V for the A10B Fab immobilized Au surface. These data further confirm that A10B scFv-cys was immobilized on the gold surface through its cysteine linker while A10B Fab-SH was immobilized on the gold surface through the sulfhydryl group.

The surface coverage of the A10B scFv-cys and Fab-SH can be calculated by integration of the stripping current peak at  $-0.93$  V (Figure 8). From the Faraday law— $Q = -nFN$ , where  $n$  = number of electrons;  $F$  = Faraday constant, 96 485 C/mol; and  $N$  = number of moles of electroactive species—we obtain a surface coverage of  $(1.74 \pm 0.53) \times 10^{-10}$  mol/cm<sup>2</sup> ( $n = 3$ ) with the scFv-cys and  $2.9 \times 10^{-11}$  mol/cm<sup>2</sup> with Fab-SH. In previously published studies,<sup>26</sup> average surface coverages of  $1.7 \times 10^{-11}$  and  $5.3 \times 10^{-12}$  mol/cm<sup>2</sup> have been reported for Fab-SH fragment-modified and whole antibody-modified surfaces, respectively. By comparison, surfaces modified with scFv-cys contain nearly 10 times as many variable antigen-binding sites per square centimeter as those modified with Fab-SH fragments, and 35 times as many as surfaces modified with whole antibody. Using scFv-cys thus markedly increases the antigen-binding-site density on the sensor surface, an especially important parameter for detecting low concentrations of antigen in complex samples.<sup>27</sup>

## Rabbit Serum Analysis

The scFv-cys PZ can identify and quantify analyte in complex biological samples. Rabbit serum was diluted and spiked with known concentrations of rabbit IgG and analyzed using the scFv-cys PZ calibration curve (Figure 6b). From the curve, the concentration of rabbit IgG was estimated to be  $11.5 \pm 0.8$  mg/mL ( $n = 3$ ). When analyzed by ELISA, the same batch of sample yielded a concentration of  $9.5 \pm 0.7$  mg/mL ( $n = 3$ ). Results from the analysis of rabbit serum by the scFv-cys PZ therefore correlated well with ELISA results.

## CONCLUSION

We have demonstrated in this study that it is possible to modify scFv's so that they form a uniform, densely packed SAM on the surface of a QCM for detection of antigen. To our knowledge, this is the first published report concerning the use of scFv with a covalent cysteine linker to create a PZ. Our experimental results have confirmed that antigen binding occurs in a concentration-dependent manner over a range of  $1.7 \times 10^{-9}$  to  $6.6 \times 10^{-8}$  M. Our study shows that the scFv-cys PZ has significant advantages regarding sensitivity and specificity compared to other types of PZs using antibody Fab fragments, Fab-SH fragments, and whole antibody. The feasibility of using scFv-cys PZ for detection of antigens in serum was tested, and results indicated that these biosensors were sufficiently sensitive to detect antigen binding in a highly complex aqueous medium. The advantages implicit in combining the highly sensitive microbalance with highly selective recombinant antibodies can lead to the rapid development of a wide range of biosensors with diagnostic potential. With current antibody phage display technology and existing scFv phage display libraries, it should be possible to rapidly identify high-affinity scFv's to a multitude of antigens and, using their propensity for self-assembly on microbalance surfaces, prepare appropriate biosensors for antigen detection in biological samples. We envision that applications of scFv's as the molecular recognition components are also beneficial for other nonlabeled detection techniques.

## ACKNOWLEDGMENT

This research was supported by the NIH (Grants 1R21EB000-672-01, 4R33EB000672-02, 5P30 CA68485-07, and 5P30 ES00267-36); the Merck/AAAS Interdisciplinary Research Program; the Oakland University Research Excellent Fund; and faculty start-up funds. We thank Michael Hartzler for his donations of fresh rabbit serum; Jennie Froelich and Brit Ranson for their hard work and innumerable hours in the laboratory; Art Bull and Denis Callewaert for their helpful discussions; and Glenda Mernaugh, Stanley Bruckenstein, and Paul McBride for their critical reading of the manuscript.

## References

1. Lew AM. *J. Immunol. Methods* 1984;72:171–176. [PubMed: 6205095]
2. Suleiman A, Guilbault GG. *Analyst* 1994;119:2279–2282. [PubMed: 7872482]
3. Sauerbrey G. *Z. Phys* 1959;155:206–222.
4. Janshoff A, Galla H, Steinem C. *Angew. Chem., Int. Ed* 2000;39:4004–4032.
5. Prime KL, Whitesides GM. *J. Am. Chem. Soc* 1993;115:10714–10721.
6. Janshoff A, Steinem C. *Sens. Update* 2001;9:313–354.
7. Su X, Chew FT, Li FY. *Anal. Sci* 2004;16:107–114.
8. Davis KA, Leary TR. *Anal. Chem* 1989;61:1227–1230. [PubMed: 2757206]
9. Vikholm I, Albers WM. *Langmuir* 1998;14:3865–3872.
10. Bird RE, Hardman KD, Jacobson JW, Johnson S, Kaufman BM, Lee SM, Lee T, Pope SH, Riordan GS, Whitlow M. *Science* 1988;242:423–426. [PubMed: 3140379]
11. Huston JS, Levinson D, Mudgett-Hunter M, Tai MS, Novotny J, Margolies MN, Ridge RJ, Brucoleri RE, Haber E, Crea R. *Proc. Natl. Acad. Sci. U.S.A* 1988;85:5879–5883. [PubMed: 3045807]
12. Padlan EA. *Mol. Immunol* 1994;31:169–217. [PubMed: 8114766]

13. The peptide mass from the A10B sequence is approximately 26443.57 Da, [au.expasy.org/cgi-bin/peptide-mass.pl](http://au.expasy.org/cgi-bin/peptide-mass.pl).
14. (a) Stayton PS, Olinger JM, Jiang M, Bohn PW, Sligar SG. *J. Am. Chem. Soc* 1992;114:9298–9299. (b) Vigmond SJ, Iwakura M, Mizutani F, Katsura T. *Langmuir* 1994;10:2860–2862. (c) Ferretti S, Paynter S, Russell D, Sapsford KE. *Trends Anal. Chem* 2000;19:530–540. (d) Lillo AM, Sun C, Gao C, Ditzel H, Parrish J, Gauss C, Moss J, Felding-Habermann B, Wirsching P, Boger DL, Janda K. *Chem. Biol* 2004;11:897–906. [PubMed: 15271348]
15. (a) Zhang Y, Telyatnikov V, Sathe M, Zeng X, Wang PG. *J. Am. Chem. Soc* 2003;125:9292–9293. [PubMed: 12889948] Finklea, HO. *Encyclopedia of Analytical Chemistry*. Meyers, RA., editor. Chichester, U.K: John Wiley & Sons Ltd.; 2000. p. 1-26.
16. Harlow, E.; Lane, D. *Antibodies: A Laboratory Manual*. Cold Spring Harbor, NY: Cold Spring Harbor Laboratory; 1988. p. 300
17. Hewing EE, Mernaugh R, Edl J, Cao P, Cover TL. *Infect. Immun* 2004;72:3429–3435. [PubMed: 15155649]
18. Biebuyck HA, Whitesides GM. *Langmuir* 1993;9:1766–1770.
19. Harlow, E.; Lane, D. *Antibodies: A Laboratory Manual*. Cold Spring Harbor, NY: Cold Spring Harbor Laboratory; 1988. p. 626-629.
20. Huang TT, Sturgis J, Gomez R, Geng T, Bashir R, Bhunia KA, Robinson PJ, Ladisch RM. *Biotechnol. Bioeng* 2003;81:618–624. [PubMed: 12514811]
21. Daniels PB, Deacon JK, Eddowes MJ, Pedley DG. *Sens. Actuators* 1988;11–18.
22. (a) Ebara Y, Itakura K, Okahata Y. *Langmuir* 1996;12:5165–5170. (b) Okahata Y, Natsuura K, Ito K, Ebara Y. *Langmuir* 1996;12:1023–1026.
23. Ngeh-Ngwainbi J, Suleiman AA, Guilbault GG. *Bioelectronics* 1990;5:13–26.
24. Schmitt N, Tessier L, Watier H, Patat F. *Sens. Actuators, B* 1997;43:217–223.
25. Su X, Chew F, Li S. *Anal. Biochem* 1999;273:66–72. [PubMed: 10452800]
26. O'Brien JC, Jones VW, Porter MD. *Anal. Chem* 2000;72:703–710. [PubMed: 10701253]
27. Lew AM. *J. Immunol. Methods* 1984;72:171–176. [PubMed: 6205095]

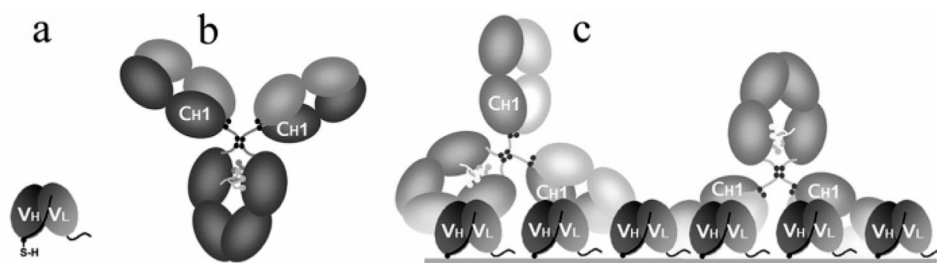


**Figure 1.**

(a) A10B-scFv with a cysteine residue incorporated into the linker. A10B-scFv recognizes the constant heavy chain 1 (C<sub>H</sub>1) domain of rabbit IgG. (b) Rabbit IgG with the C<sub>H</sub>1 domain labeled. (c) Schematic of the interaction between anti-rabbit scFv's covalently bound to the gold surface of a QCM through the incorporated cysteine and rabbit IgG.

1 MAQVQLQQSG TEVVKPGASV KLSCKASGYI FTSYDIDWVR QTPEQGLEWI 50  
51 GWIFPGEGST EYNEKFKGRA TLSVDKSSST AYMELTRLTS EDSAVYFCAR 100  
101 GDYRRYFDL WGQTTVTVS SGGGSGGGG SGGGSDIEL TQSPTIMSAS 150  
151 PGERVTMTCS ASSSIRYIW YQKPGSSPR LLIYDTSNVA SGVPSRFSGS 200  
201 GSGTSYSLTI NRMEAEDAAT YYQEWSGYP YTFGGGKLE LKQAAAGAPV PYPDPLEPRAA 250

**Figure 2.**

Whole amino acid sequences of the modified single-chain antibody A10B210E derived from an A10Br mouse hybridoma clone. Underlined is the incorporated E-tag.



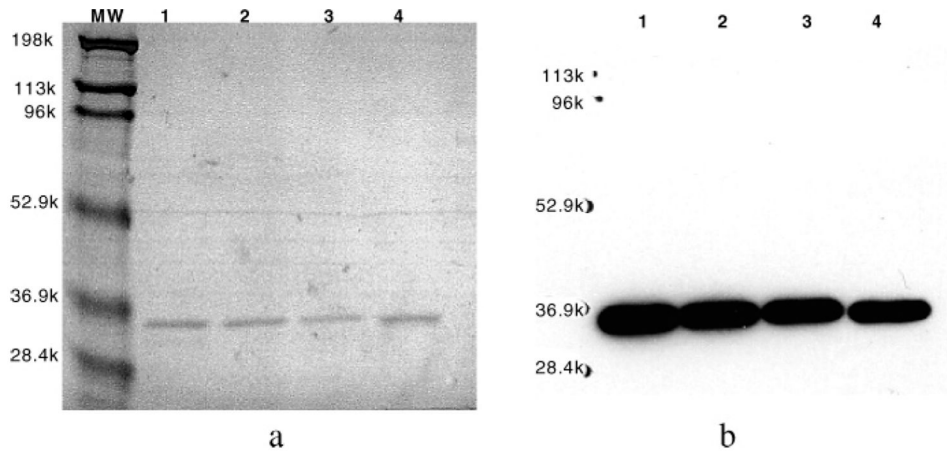


**Figure 3.** SDS-PAGE and Western blot analysis of A10B scFv: affinity-purified A10B scFv (lanes 1–3) and scFv-cys (lane 4) preparations assayed by Coomassie-stained SDS-PAGE (a) and HRP/anti-E-tag Western blot analysis (b).

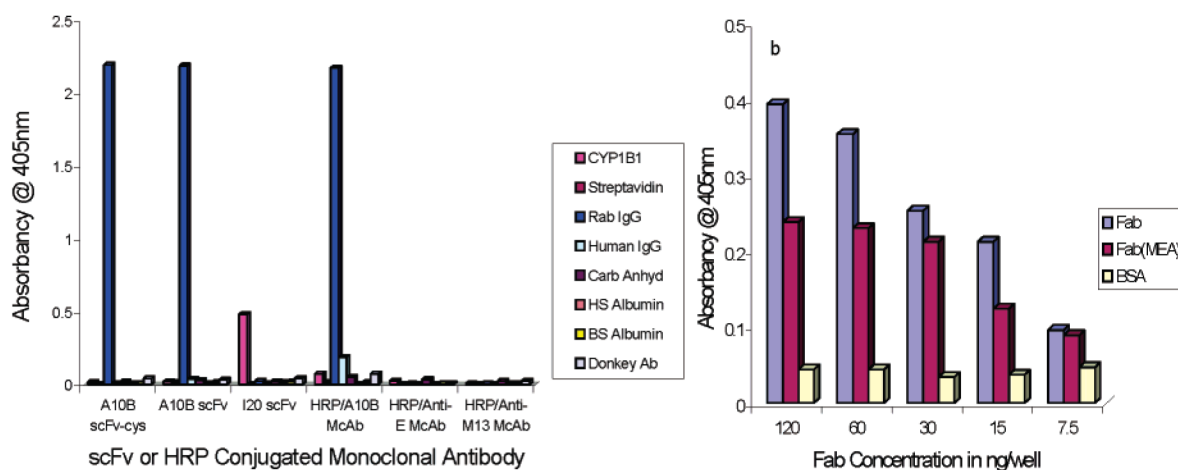


**Figure 4.** Characterization of A10B monoclonal, Fab fragment, and scFv antibodies by ELISA. (a) ELISA results for HRP/A10B monoclonal, A10B scFv, A10B scFv-cys, and negative control (HRP/anti-E and HRP/anti-M13 monoclonal and I20 scFv) antibodies on rabbit IgG, CYP1B1, streptavidin, human IgG, carbonic anhydrase, human serum albumin, bovine serum albumin, and donkey antibody. (b) ELISA results for varying concentrations of A10B Fab fragments reduced with MEA or nonreduced on rabbit IgG or BSA.

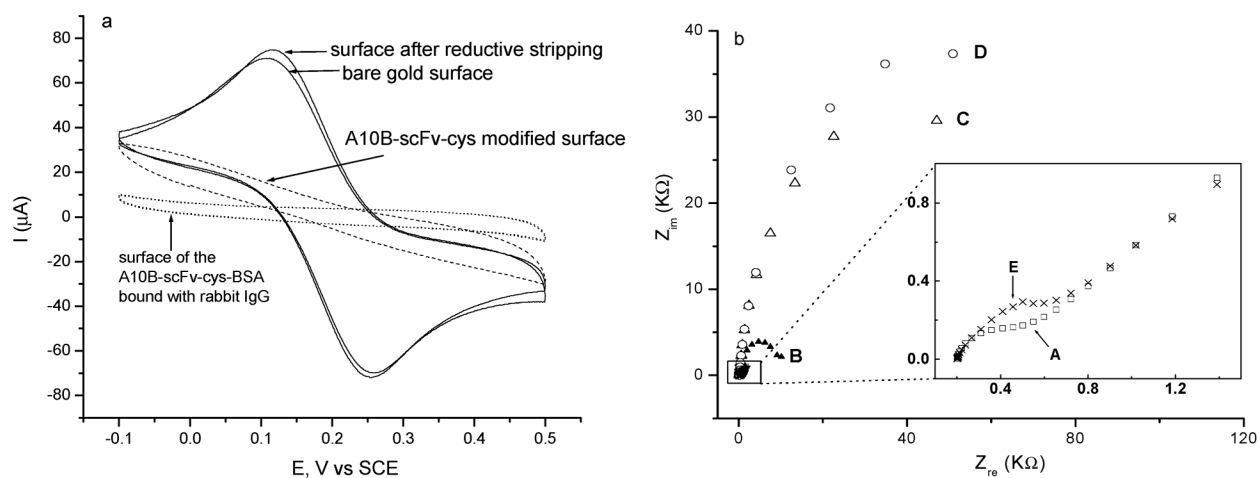


**Figure 5.**

(a) Cyclic voltammograms, scan rate 100 mV/s. (b) Nyquist plots in a solution of 0.1 M  $\text{NaClO}_4$  containing 1 mM  $\text{K}_4\text{Fe}(\text{CN})_6/\text{K}_3\text{Fe}(\text{CN})_6$ . Curve A, the bare gold electrode ( $\square$ ); curve B, scFv-cys-modified gold electrode ( $\blacktriangle$ ); curve C, scFv-cys-modified gold electrode blocked with BSA ( $\triangle$ ); curve D, scFv-cys-BSA-modified gold electrode incubated with rabbit IgG ( $\circ$ ); curve E, scFv-cys-BSA-modified gold electrode after removal of the scFv monolayer by reductive stripping in 0.5 M KOH ( $\times$ ).

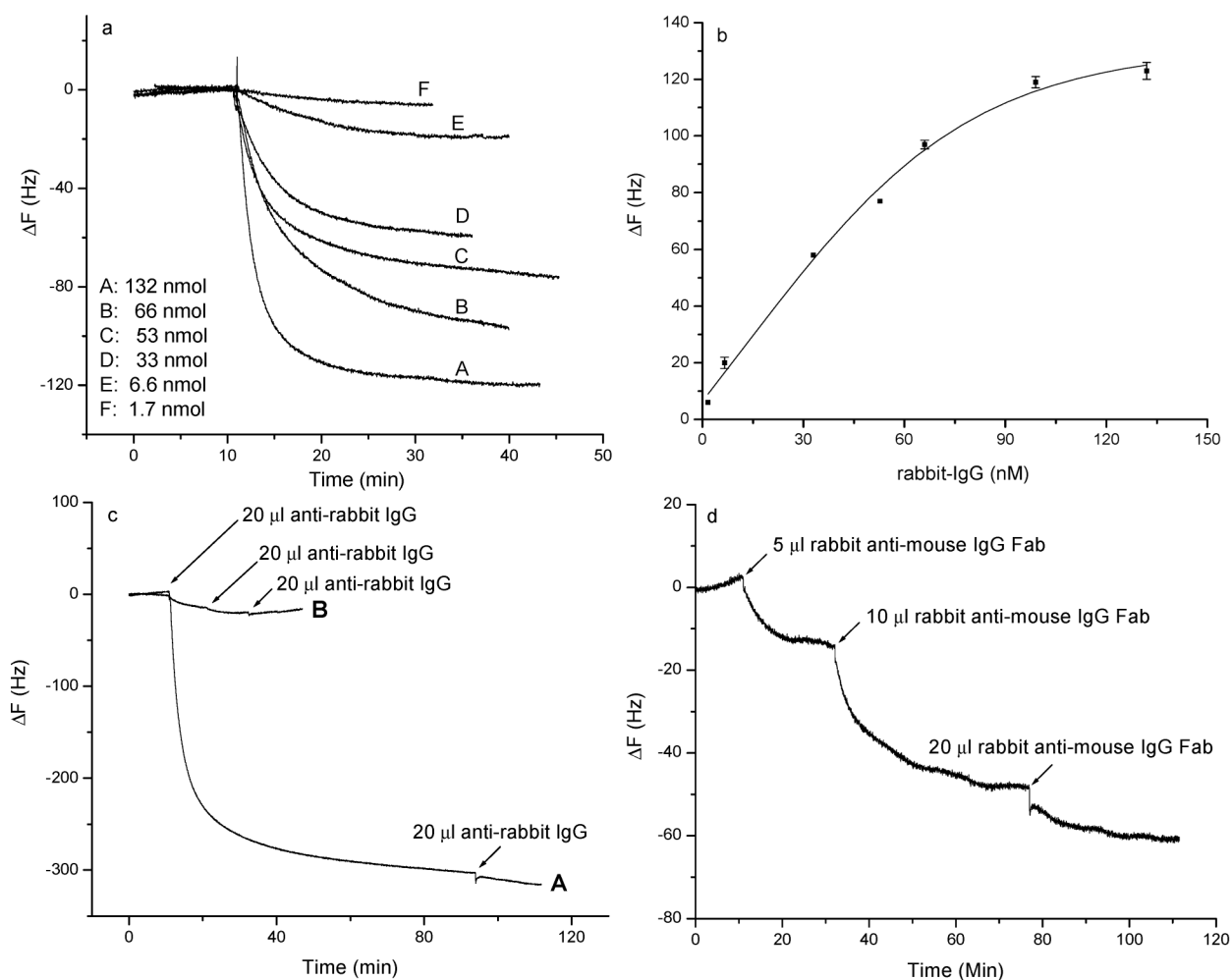


**Figure 6.**

(a) Frequency change vs time for scFv-cys PZs in the presence of various concentrations of rabbit IgG in PBS. Rabbit IgG was added in 20- $\mu$ L aliquots to an A10B scFv-cys-modified gold QCM electrode in 1 mL of PBS. (b) Relationship between the frequency change and concentration of rabbit IgG. (c) Effect of secondary antibody (i.e., goat anti-rabbit IgG) binding to rabbit IgG captured by scFv-cys. Curve A: frequency change in response to the addition of an aliquot of  $3.3 \times 10^{-6}$  M anti-rabbit IgG. Rabbit IgG was first bound to an A10B scFv-cys-modified biosensor in 1 mL of PBS, followed by addition of polyclonal goat anti-rabbit IgG. Curve B: negative control where only polyclonal goat anti-rabbit IgG was added to the A10B scFv-cys immobilized QCM biosensor. The electrode was washed with biograde water and PBS and then dried before addition of the anti-rabbit IgG. (d) Frequency change vs time curve when successive volumes (i.e., 5, 10, and 20  $\mu$ L) of  $1.3 \times 10^{-5}$  M rabbit IgG Fab fragments were added to the A10B scFv-cys immobilized Au QCM electrode in 1 mL of PBS buffer.

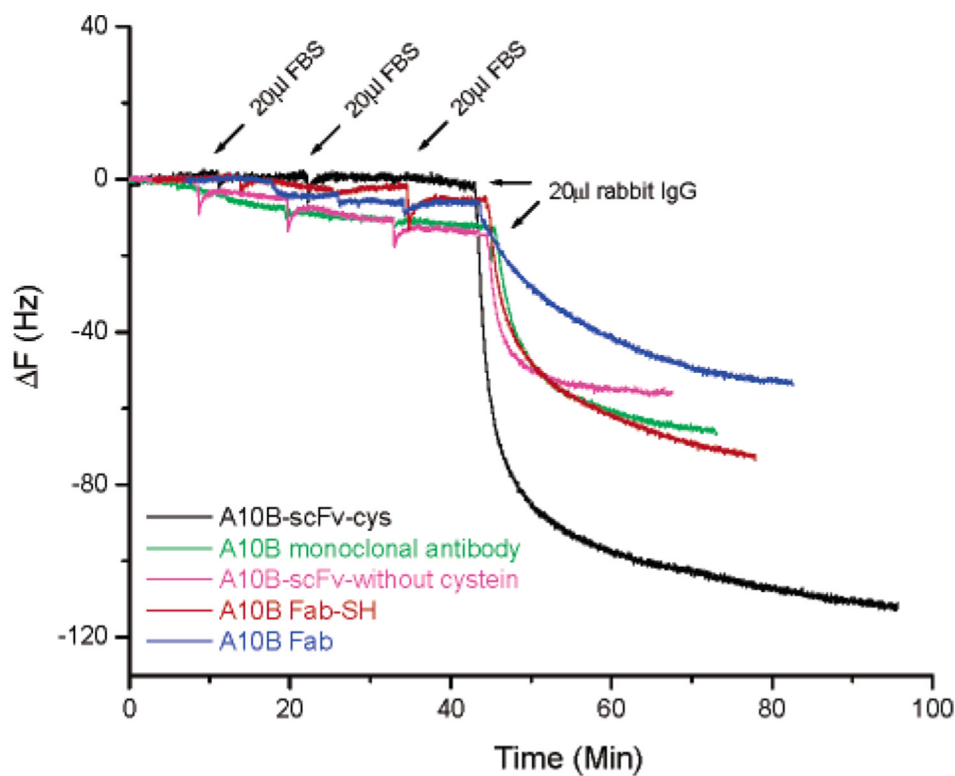


**Figure 7.** Comparison of sensor selectivity and sensitivity for PZs generated with A10B scFv-cys (black), A10B monoclonal antibody (green), A10B-scFv without cysteine linker (purple), A10B Fab (blue), or A10B Fab-SH (red). For each PZ, 20  $\mu$ L of FBS (0.36 mg/mL) was added three times to 1 mL of PBS buffer. This was followed by the addition of 20  $\mu$ L of rabbit IgG (1 mg/mL) to 1 mL of PBS buffer, evaluating antigen detection in a complex matrix. The final concentration of rabbit IgG is 132 nM.



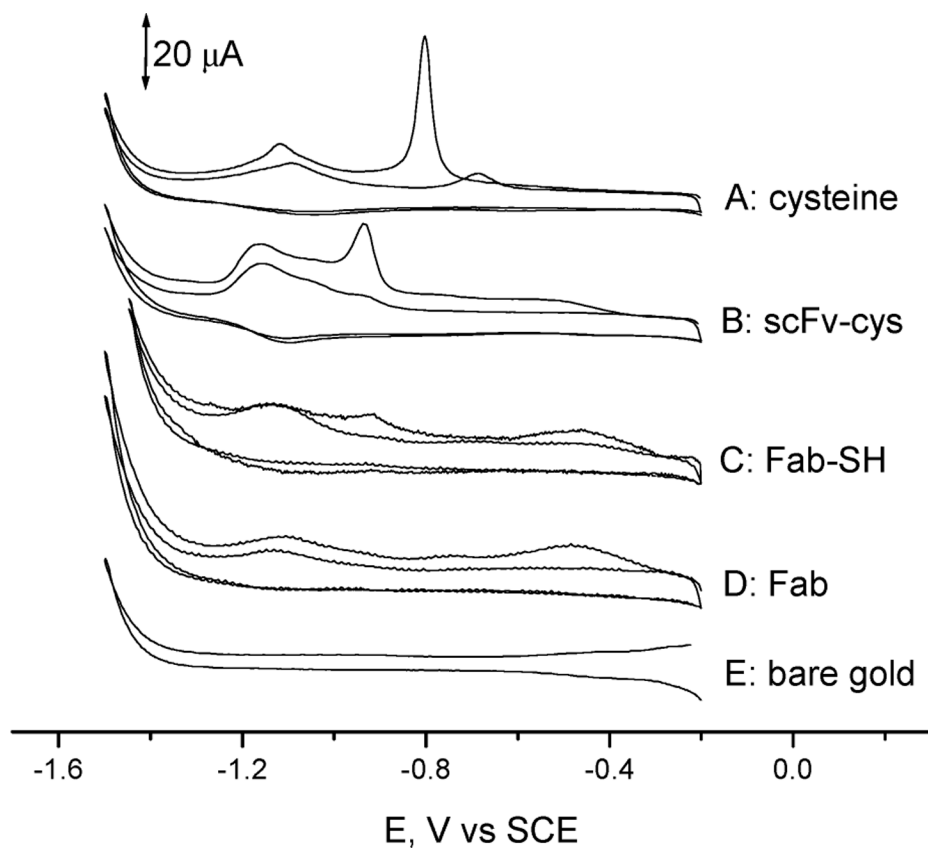


**Figure 8.** Cyclic voltammograms obtained in 0.5 M KOH aqueous solution at a scan rate of 100 mV/s. Dissolved oxygen was removed by a 15 min nitrogen purge. Two cycles are shown. Key: curve A, cysteine-modified gold electrode; curve B, scFv-cys-modified gold electrode; curve C, Fab-SH-modified gold electrode; curve D, Fab-modified gold electrode; curve E, bare gold electrode. The counter electrode is a platinum wire. Only two scans are shown for clarity of presentation.

**Table 1**  
Changes in Damping Resistances for Experiments Shown in Figure 6 and Figure 7

	$ \Delta R_q /R_q(\%)$		$ \Delta R_q /R_q(\%)$
Figure 6a, curve A	0.5	Figure 6c, curve A	0.7
Figure 6a, curve B	0.5	Figure 6c, curve B	1.0
Figure 6a, curve C	0.4	Figure 7, black	0.5
Figure 6a, curve D	0.1	Figure 7, green	0.3
Figure 6a, curve E	0.1	Figure 7, purple	0.5
Figure 6a, curve F	0.4	Figure 7, red	0.4
Figure 6d	0.2	Figure 7, blue	0.3